Journal of Environmental Sciences Vol.15, No.4, pp.456—463, 2003

ISSN 1001—0742
CN11—2629/X

Article ID: 1001-0742(2003)04-0456-08 **CLC number**: X13 **Document code**: A

Spectroscopic study on variations in illite surface properties after acid-base titration

LIU Wen-xin[1,*], COVENEY R. M.[2], TANG Hong-xiao[1]

(1. SKLEAC, Research Center for Eco-Environmental Sciences, Chinese Academy of Sciences, Beijing 100085, China. E-mail: wxliu@urban.pku.edu.cn; 2. Department of Geosciences, University of Missouri-Kansas City, 420D Robert H. Flarsheim Hall, 5100 Rockhill Road, Kansas City, Missouri 64110-2499)

Abstract: FT-IR, Raman microscopy, XRD, ^{29}Si and ^{27}Al MAS NMR, were used to investigate changes in surface properties of a natural illite sample after acid-base potentiometric titration. The characteristic XRD lines indicated the presence of surface Al-Si complexes, preferable to $Al(OH)_3$ precipitates. In the microscopic Raman spectra, the vibration peaks of Si-O and Al-O bonds diminished as a result of treatment with acid, then increased after hydroxide back titration. The varied ratio of signal intensity between ^{IV}Al and ^{VI}Al species in ^{27}Al MAS NMR spectra, together with the stable BET surface area after acidimetric titration, suggested that edge faces and basal planes in the layer structure of illite participated in dissolution of structural components. The combined spectroscopic evidence demonstrated that the reactions between illite surfaces and acid-leaching silicic acid and aluminum ions should be considered in the model description of surface acid-base properties of the aqueous illite.

Keywords: natural illite; acid-base titration; spectroscopic information; surface Al-Si species; surface complexation

Introduction

During dissolution and formation of clay minerals, the dominant solutes are hydrolyzed aluminum ions, silicic acid and the reacted product—hydroxyaluminosilicates (HAS). HAS can easily generate at ambient temperature over the pH range of 4 to 7, and significantly affect the distribution and bioavailability of aluminum (Browne, 1992; Farmer, 1994). On the other hand, the influence of natural particles, as the reaction substrate, should be considered, due to surface complexation or precipitation with components in aqueous medium (Lu, 1996). Usually, observation of natural particles on the molecular scale is resolved with various spectroscopic probes. Illite is the main constituent of most shale, the single most abundant sedimentary rock type, and has been the subject of many studies (Sinitsyn, 2000; Kulik, 2000). However, there have been few direct microscopic investigations into the corresponding changes of illite surface properties caused by acid-base titration and identification of surface products with combined spectroscopic methods.

In the current study, *X*-ray diffraction (XRD), Fourier transform infrared spectrometry (FT-IR), microscopic Raman spectrometry, and solid state ^{29}Si and ^{27}Al nuclear magnetic resonance (NMR) are employed to investigate the variations in surface properties of a natural illite after acid-base potentiometric titration. The spectroscopic evidence, at the molecule level, would facilitate verification of the model description of surface reactions at the surface sites of illite (Liu, 1999).

1 Material and methods

1.1 Materials

A natural illite was collected from Williams Town (WT), South of Australia. The initial sample was ground and sieved to less than 53 μm fractions. Then, three sub-samples were individually made as followed:

1.1.1 Hydrated sample

After two weeks of equilibration at 4℃, a suspension of 10 g/L was centrifuged at 20000 r/min, 10℃

Foundation item: The National Natural Science Foundation of China (No. 20037010). * Corresponding author. Present address: College of Environmental Sciences, Peking University, Beijing 100871, China

for 30 min. The separated solid was dried at 60℃ for 12 h and ground to a powder. Soluble components in the residual aqueous phase, as the neutral supernatant, were measured.

1.1.2 Acidified sample

A suspension of 10 g/L in 0.1 mol/L $NaNO_3$ was prepared and titrated using a standard 0.1 mol/L HNO_3 solution. In this study, pH 4 was adopted as the end-point of the acidimetric titration. The defined equilibrium criterion during potentiometric titration under magnetic stirring was the drift of potential reading, after each addition of titrant, below 1 mV/h at 25℃ (with oil thermostat) in a N_2 atmosphere. Then, the same centrifugation was applied to the sample. The acidimetric supernatant was regarded as the system blank of potentiometric titration to examine the dissolution extent of illite matrix.

1.1.3 Back titrated sample

Based on the foregoing acidimetric titration, a subsequent back titration was conducted up to around pH 5.5 by dripping a standard 0.05 mol/L NaOH solution. The suspension was then stabilized for 24 h before solid-aqueous separation. No further rinsing step was utilized for the acidimetric and alkalimetric samples to avoid possible disturbance.

The specific external surface area was determined by the N_2/BET method(Micrometrics, ASAP Model 2000). Chemical compositions of primary solids and dissolved components of two supernatants were analyzed by inductively coupled plasma-atomic emission spectrometry (ICP-AES, ARL Model 3580). The image of the sample was examined by scanning electron microscope(SEM, Philips, XL 30), which showed plate-like crystals stacked in the layer structure of typical sheet silicates (Fig.1).

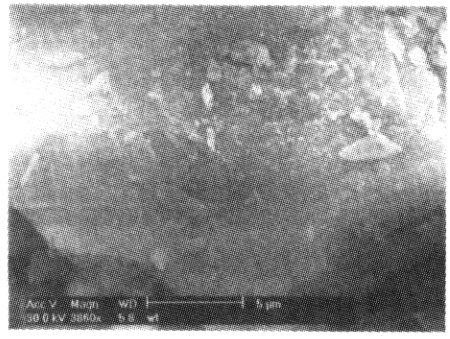

Fig. 1 Scanning electron microscopy (SEM) of the illite(the scale was 5 μm)

1.2 Spectroscopic determinations

1.2.1 FT-IR

A 1 mg sample was mixed with 100 mg KBr (spectroscopic grade, oven-dried at 110℃ overnight). All spectra, using the diffuse reflectance infrared Fourier transform(DRIFT) technique, were recorded on a Perkin-Elmer FT-IR 2000X spectrometer with a spectral resolution of 4 cm^{-1}. 200 scans were averaged for each measurement from 370 to 4000 cm^{-1}.

1.2.2 Microscopic Raman

At room temperature, a Renishaw 1000 microprobe system with a detector of charge coupled device (CCD) was utilized to detect the Raman spectra excited by a Spectra-Physics Model 127 He-Ne laser(633 nm). The powdered sample was fixed on the stage of a microscope equipped with a 50 × objective lens (Olympus BHSM). The scanning limits were 100—2000 cm^{-1} with a resolution of 2 cm^{-1}. 25 acquisitions with a detection time of 8—10s were made. All spectra were calibrated using the 520 cm^{-1} line of a silicon wafer. The detection procedure was repeated in different areas to reduce possible deviation.

1.2.3 Powder XRD

Powder *X*-ray diffractometry (Siemens, Model D5000) was conducted with Cu Kα radiation at a scanning rate of 0.02°s^{-1}. The diffraction profiles with a 0.001 nm precision of the d-spacing measurement were reproducible in the region of 5° and 85°2θ.

1.2.4 Solid state NMR

Multinuclear solid state NMR spectra were acquired at room temperature using a CMX360

spectrometer(8.45 Tesla, Chemagnetics). All solid samples were separately packed into magic angle spinning(MAS) rotors(diameter = 7 mm) sealed with end caps. The acquisition conditions for ^{29}Si and ^{27}Al are listed in Table 1.

Since a preceding test for cross-polarization (CP) with ^{1}H showed no apparent improvement on the signal enhancement for ^{29}Si NMR, the CP technique was not adopted for the actual measurements.

Table 1 Experimental conditions of ^{27}Al and ^{29}Si solid state NMR

Nuclei	^{27}Al	^{29}Si
Resonance frequency, MHz	93.795	71.508
90° pulse width(μs) / interval(s)	2.4/2	4.5/2
Acquisition time (ms) / delay(μs)	41/20	68/25
Spinning speed, kHz	7.0	6.0
Accumulation number	128—1024	900—3000
External reference for chemical shift, ppm	1.0 mol/L $Al(H_2O)_6Cl_3$	Tetramethylsilane (TMS)

2 Results

2.1 Compositions of solids and supernatants

Main constituents in the primary solid, as well as concentrations of soluble components in the neutral supernatant and in the acidimetric supernatant, are presented in Table 2. The results indicate that solid dissolution at neutral pH is minimal, whereas the acidimetric titration significantly facilitates the release of structural components(e.g., Si and Al), though the dissolution is non-stoichiometric based on crystallography.

Table 2 Solid constituents (mean ± one standard deviation) and main dissolved components in neutral and acidimetric supernatants of the illite sample

Main components	Weight percentage
SiO_2	55.7 ± 0.3
Al_2O_3	28.9 ± 0.5
K_2O	6.9 ± 0.2
Final pH in the supernatants ICP-AES measurements	pH 7.3[n]/pH 4.1[a]
Si^n/Si^a ($\times 10^{-4}$ mol/L)/%[b]	3.7/10.1/0.7
Al^n/Al^a ($\times 10^{-4}$ mol/L)/%[b]	0.3/5.9/0.6
K^n/K^a ($\times 10^{-4}$ mol/L)/%[b]	2.2/60.6/43.2
BET surface area, m^2/g	19.04 ± 0.05[c]/19.01 ± 0.11[d]
Basal d(001) value, nm	0.991 ± 0.001

Notes: [n]——neutral supernatant; [a]——acidimetric supernatant; [b]——acidic dissolution extent of solid mass (10 g/L × 0.05 L); [c]——particle surface area in the neutral suspension; [d]——particle surface area in the acidimetric suspension

2.2 FT-IR

Typical FT-IR spectra of samples after acid-base treatments are illustrated in Fig.2. The vibrational assignment of major functional groups is listed in Table 3.

Due to relatively weak detachment of main structural elements (less than 1% for Si and Al, Table 2), the influence of acidic titration on the bulk configuration of the natural illite appears to be insignificant. This case is also indicated by lack of remarkable changes in the IR vibrational intensity and by absence of band position shift. On the other hand, a new absorption band presented at 1385 cm^{-1} after acid-base potentiometric titration. Two possible explanations correspond to this situation: one is the residual NO_3^- after solid-solution separation, originated from 0.1 mol/L $NaNO_3$ and from addition of 0.1 mol/L HNO_3 during the acidimetric titration, the other is attributed to the $\nu 3$ vibrations of nitrate group(Nakamoto, 1997). In the latter case, the nitrate group may act as the outer-sphere counter-ions for charge neutrality in the composition of the surface solid species carrying positive charges, such as Al-Si complexes at the illite

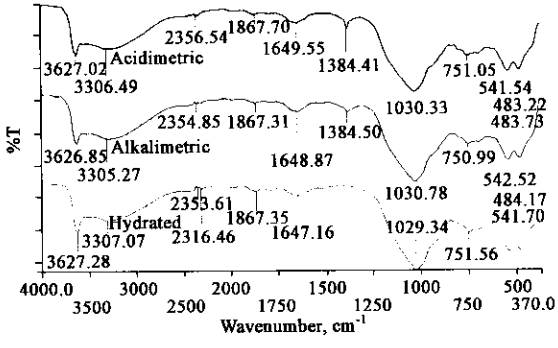

Fig.2 FT-IR spectra of the samples

surface sites. It is also confirmed by the recent results, in which the presence of nitrate anion affected the local structure of the synthetic amorphous aluminosilicates, and changed their surface charge and adsorption capacity(Miyazaki, 1999).

Table 3 Assignment of IR and Raman vibrations for the illite sample

IR peak maxima, cm^{-1}	Assignment
3600—3630	Inner OH stretching motions, e.g., Mg_2OH, Al_2OH (Farmer, 1974)
3300—3350	Vibrations of organic matter (Farmer, 1974)
1610—1650	HOH bending (water molecule) vibrations (Farmer, 1974)
1370—1385	$\nu3$ vibrations of NO_3^- groups (Nakamoto, 1997)
1010—1030	Si-O stretching in-plane (Si-O-Si) vibrations (Farmer, 1974; Komadel, 1996)
915—950	Al_2OH in-plane vibrations (Farmer, 1974)
750	Al-O-Si in-plane vibrations (Farmer, 1974)
600—700	OH bending vibrations (Farmer, 1974)
400—550	Si-O (or Si-O-Al) bending in-plane vibrations (Farmer, 1974; Komadel, 1996)
Raman peak maxima, cm^{-1}	**Assignment**
1000—1100	Asymmetric vibrations of Si-O-Si (Lazarev, 1972; Nakamoto, 1997)
650—750	Al-O vibrations (Lazarev, 1972; Nakamoto, 1997)
450—550	Symmetric vibrations of Si-O-Si (Lazarev, 1972; Nakamoto, 1997)
750—830	$\nu1$ (A1) vibrations of SiO_4 unit (Nakamoto, 1997)
300—400	$\nu2$ (E) vibrations of SiO_4 unit (Nakamoto, 1997)
800—1000	$\nu3$ (F2) vibrations of SiO_4 unit (Nakamoto, 1997)
450—600	$\nu4$ (F2) vibrations of SiO_4 unit (Nakamoto, 1997)

2.3 Raman spectroscopy

Since the spectrometer eliminated the Rayleigh line close to 150 cm^{-1}, interpretation of bands below 200 cm^{-1} was disregarded due to poor reliability. Assignment of Raman vibrations is listed in Table 3.

Fig. 3 depicts the microscopic Raman spectra of the illite samples prior to and after each stage of the acid-base titration. Compared to the hydrated sample, acidimetric and alkalimetric titration respectively induced diminishment and certain resumption of the scattered intensity of symmetric bending vibrations of Si-O bond near 465 cm^{-1}. Similar situation was also found in the region of Al-O bond vibrations at 650—750 cm^{-1}.

Consequently, the spectral information indicates that some products with Al-O-Si structural components were created on the illite surfaces during the hydroxide back titration, probably resulted from the interactions between soluble Al species and silicic acid, which generated from acidic disassociation of the illite substrate.

2.4 XRD traces

The alterations of the illite samples caused by acid-base titration are displayed in Fig. 4 after background subtraction, Kα2 stripping and Fourier expansion.

Following acidimetric titration, heights of the diagnostic 00*l* diffraction lines of the natural illite (Srodon, 1984) dramatically decreased with respect to those of the hydrated sample. This situation is similar to that reported by Komadel *et al.* (Komadel, 1990). The signal intensities of some diffraction peaks, especially at 26.5°2θ with a *d*-value of 0.334—0.337 nm, rose again after hydroxide back titration up to about pH 5.5. Compared with the standard diffraction patterns in

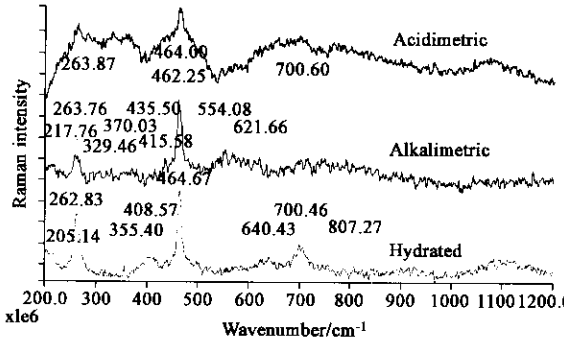

Fig. 3 Microscopic Raman spectra of the samples
For simplicity and comparison, all spectra have been shown in splitting mode(i.e., displayed as an equally divided vertical stack of separate plots) and performed using auto-Y-scale manipulation. The intensity scale of the acidimetric sample has been magnified

the built-in database, the matching results indicate the formation of Al-Si complexes or precipitates at the illite surfaces, preferable to bulk $Al(OH)_3$ (e.g., bayerite or nordstrandite), which validates, in a sense, the mechanistic interpretation that the presence of silicic acid can inhibit the nucleation of solid $Al(OH)_3$ (Exley, 1993).

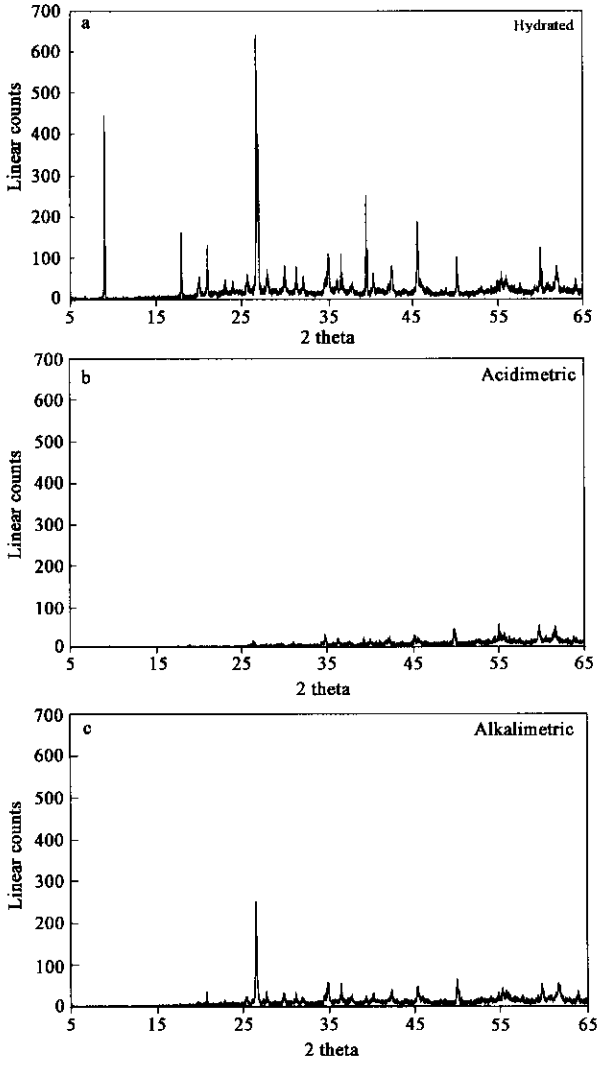

d(*hkl*) (Srodon, 1984)	*d*(001)	*d*(002)	*d*(020 or 110)
2θ angle	9°	18°	20°
d(*hkl*) (Srodon, 1984)	*d*(111)	*d*(003 or 022)	*d*(200 or 131)
2θ angle	21°	26.5°—27°	35°

Fig.4 Powder XRD profiles. The incorporated table lists the prominent diagnostic reflection of the natural illite

2.5 Solid state MAS NMR

2.5.1 ^{29}Si NMR spectra

The corresponding assignments of ^{29}Si and ^{27}Al resonance are listed in Table 4. Fig. 5 portrays the ^{29}Si MAS NMR spectra of the illite samples.

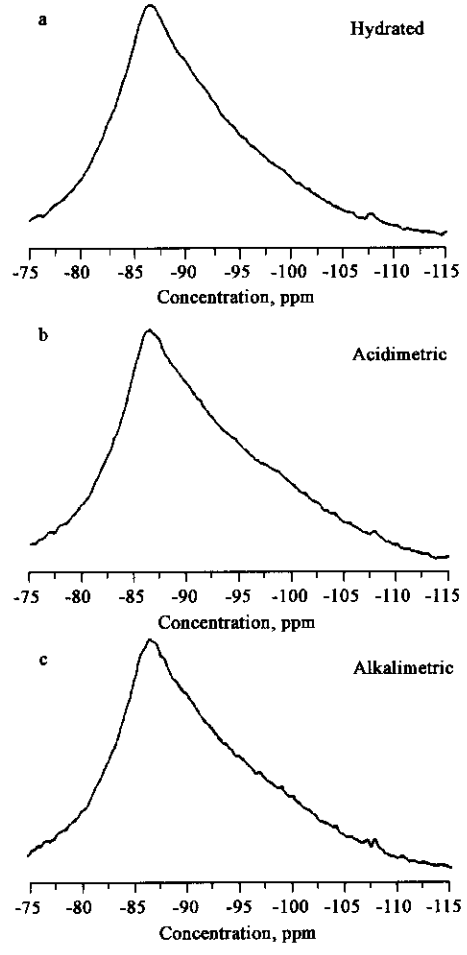

Fig.5 Solid state ^{29}Si MAS NMR spectra of the samples

The broad peak (from − 80 to − 100 ppm), centered at − 86.5 ppm, was formed by the overlap of some Q^3 *m*Al structural units (Table 4), and reflected a wide range of substitution patterns of ^{IV}Al for Si(Smith, 1983; Kinsey, 1985). Moreover, the resonant signal at − 108.5 *ppm was associated with a quartz impurity* (*Tkàc*, 1994).

Table 4 Signal assignments of NMR resonance of different nuclei

Nuclei	Assignment				
^{29}Si	Quartz	$Q^3 0Al^*$ (smectite)	$Q^3 0Al^*$	$Q^3 1Al^*$	$Q^3 2Al^*$
Chemical shift δ_{iso}, ppm (Kinsey, 1985; Lausen, 1999; Tkàc, 1994; Weiss, 1987)	-108.5	-94.2	-89.5	-86.5	-83
^{27}Al	^{VI}Al	^{V}Al	^{IV}Al	Sidebands**	
Chemical shift δ_{iso}, ppm (Goodman, 1994; Kinsey, 1985; Lippmaa, 1986)	2.8—3.6, -10	30—31	61, 69—71	79, -73	

Notes: * The main structural units in layer silicates are presented in terms of $Q^m nAl$ ($n = 0$—3) (Kinsey, 1985; Smith, 1983). The superscript is the number of bridging oxygen atoms coordinated to a Si, and n represents the extent of tetrahedral Al substitution in the next-nearest coordination sphere (Lausen, 1999; Smith, 1983; Weiss, 1987). ** Another sideband signal is covered by ^{IV}Al resonant signals

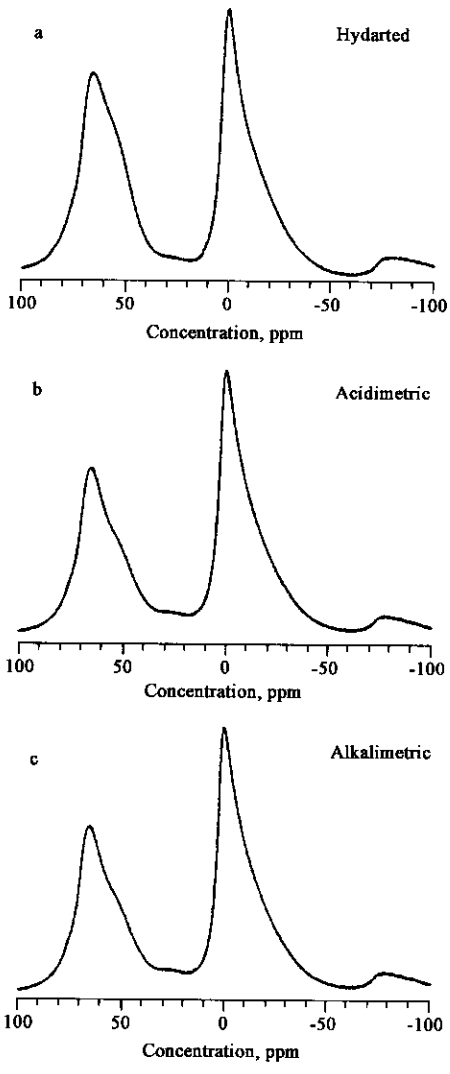

Fig.6 Solid state ^{27}Al MAS NMR spectra of the samples

In principle, variations in the structure of silicate array can be observed by ^{29}Si MAS NMR, whereas the relevant change caused by the acid-base titration can not be detected with certainty in this study, perhaps, because of poor spectral resolution or the overlap of neighboring broad resonant signals.

2.5.2 ^{27}Al NMR spectra

As to sheet clay minerals, the aluminum species are mainly composed of fourfold tetrahedral aluminum (^{IV}Al) and six-coordinated octahedral aluminum (^{VI}Al). The detailed assignment of ^{27}Al resonant signal is shown in Table 4, and the corresponding spectra of the different samples are displayed in Fig.6.

Generally speaking, 2:1 layer aluminosilicates dissolve preferentially from the edge surfaces of the crystal structure (Nagy, 1995). The decrease in NMR signal intensity of ^{IV}Al should be more difficult than that of ^{VI}Al, since the former is situated, via isomorphic substitution, in the relatively stable three-dimensional framework of silica (Tkàc, 1994). Nevertheless, the basal siloxane planes inside the layer structure are also highly reactive in the presence of structural defects (e.g., steps or kinks), isomorphic substitution, and impurities (Nagy, 1995; Komadel, 1990).

After acidimetric titration, the decreasing intensity ratio of ^{IV}Al to ^{VI}Al, in comparison with the hydrated sample (0.89 →0.67), shows that not only the edge faces but also the basal sheets in the illite crystal structure are active. This situation is in agreement with another study (Komadel, 1996). Additionally, the stable BET surface area (Table 2) partially demonstrates that the basal planes also make a contribution to the dissolution of the natural illite in this paper. Replacement of some aluminum ions, dissolved from illite substrate, for some of the silicon in the reorganized tetrahedral sheets during the hydroxide back

titration, would lead to increase in the signal intensity of ^{IV}Al. However, the reason for the close values of $^{IV}Al/^{VI}Al$ between the alkalimetric sample(0.65) and the acidimetric sample(0.67) is unclear.

Similarly, Fitzgerald *et al*. (Fitzgerald, 1992) suggested that the colloidal Al-Si precipitate mainly included the tetrahedral structural units of $Q^3 0Al$ and $Q^3 1Al$. The characteristics of ^{29}Si and ^{27}Al MAS NMR of the synthetic amorphous aluminosilicates (Miyazaki, 1999) were also analogous to those of the surface Al-Si complexes in this study.

3 Discussion

The general reaction stoichiometry for the formation of Al-Si species in synthetic or natural solutions can be expressed(Browne, 1992):

$$pAl^{3} + + qH_4SiO_4 + rH_2O \Leftrightarrow Al_p(OH)_r(OSi(OH)_3)_q^{3p-q-r} + (q+r)H^+ . \quad (1)$$

The stability test and stoichiometric calculation of the pertinent equilibrium constants indicated that hydroxyl Al-Si complexes do not play a significant role in most natural surface water(Farmer, 1994). But solid particles with widespread existence should be considered, since they probably participate, as the matrix, in the corresponding surface complexation reactions.

In a previous study(Liu, 1999), some surface reaction procedures were introduced to describe the concerned acid-base properties of the natural illites. A constant capacitance model(CCM) was employed due to its concise form and applicability to the dominant ionic strength(Lützenkirchen, 1999), like 0.1 mol/L $NaNO_3$ used in this study. Besides the proton reactions of Al^{3+} and $Si(OH)_4$ in aqueous solution, only the monomeric Al-Si complexes was considered, for simplicity, to simulate the corresponding surface processes of the illite:

$$Al^{3+} + H_4SiO_4 \Leftrightarrow Al(OSi(OH)_3)^{2+} + H^+ , \ pK_f = 2.74 \pm 0.02 \text{(Sjöberg, 1998)}, \quad (2)$$

$$\equiv SOH \Leftrightarrow \equiv SO^- + H^+ , \ pK_a^{int} = 4.04 \pm 0.01, \quad (3)$$

$$\equiv SOH + Al^{3+} + H_4SiO_4 \Leftrightarrow \equiv SOAl(OSi(OH)_3)^+ + 2H^+ , \ pK_{SC} = 3.53 \pm 0.03, \quad (4)$$

$$\equiv XH + K^+ \Leftrightarrow \equiv XK + H^+ , pK_i = 8.52 \pm 0.05. \quad (5)$$

Here, $\equiv SOH$ and $\equiv XH$ denote the amphoteric sites and the weakly acidic sites on the illite surfaces, respectively. The K_f, K_a^{int}, K_{SC} and K_i respectively represent the reaction constants of Formulae (2)—(5). The last reaction accounted for a considerable release of K^+ during the acidimetric titration (Table 2). Using the FITEQL program(Westall, 1982), the good optimization results, as indicated by the total variance($V_Y = 15.3 < 20$), substantiate the related interactions between acid-leaching components(i.e., hydrolyzed Al species and silicic acid) and illite surface sites(Liu, 1999).

By the aid of DTA-TG spectra, a recent paper revealed the formation of amorphous aluminosilicates with Si-O-Al bonds during co-precipitation of silicic acid and aluminum hydroxide in the presence of coexisting anions (Miyazaki, 1999). This phenomenon is consistent with the spectroscopic information mentioned above, where the increasing vibrational intensities of Al-O and Si-O bonds in the microscopic Raman spectra after alkalimetric titration and the matching XRD patterns, prefer the formation of surface Al-Si complexes or precipitates.

4 Conclusions

Accordingly, based on model description and combined spectroscopic evidence, acidimetric titration and subsequent formation of surface Al-Si complexes/precipitates, have an influence, at the microscopic level, on the surface acid-base chemistry of the natural illite in this paper.

Acknowledgements: Gratitude is expressed to Dr. FROST, R. Queensland University, Australia, for providing the illite sample. LIU W. X. would sincerely acknowledge Prof. FORSLING W. and Doc. SUN Z. X. of Luleå University of Technology (LTU) for their instruction and suggestion.

References:

Browne B A, Driscoll C T, 1992. Soluble aluminum silicates: stoichiometry, stability, and implications for environmental geochemistry[J]. Science, 256: 1667—1670.

Exley C, Birchall J D, 1993. A mechanism of hydroxyaluminosilicate formation[J]. Polyhedron, 12: 1007—1017.

Farmer V C, 1974. The layer silicates[M]. Infrared spectra of minerals(Farmer V. C. ed.). London: The Mineral Society. 331—362.

Farmer V C, Lumsdon D G, 1994. An assessment of complex formation between aluminum and silicic acid in acidic solutions[J]. Geochim Cosmochim Acta, 58: 3331—3334.

Fitzgerald J J, Murali C, Nebo C O *et al*., 1992. Synthesis, chemical analyses, and solid-state NMR studies of aluminum silicate hydrosols [J]. J Colloid Interface Sci, 151: 298—316.

Goodman B A, Chudek J A, 1994. Nuclear magnetic resonance spectroscopy[M]. Clay mineralogy: spectroscopic and chemical determinative methods(Wilson M. J. ed.). London: Chapman & Hall Publisher. 142—167.

Kinsey R A, Kirkpatrick R J, Hower J *et al*., 1985. High resolution aluminum-27 and silicon-29 nuclear magnetic resonance spectroscopic study of layer silicates, including clay minerals[J]. Am Mineral, 70: 537—548.

Komadel P, Schmidt D, Madejova J *et al*., 1990. Alteration of smectites by treatments with hydrochloric acid and sodium carbonate solutions [J]. Appl Clay Sci, 5: 113—122.

Komadel P, Madejova J, Janek M *et al*., 1996. Dissolution of hectorite in inorganic acids[J]. Clays Clay Minerals, 44: 228—236.

Kulik D A, Aja S U, Sinitsyn V A *et al*., 2000. Acid-base chemistry and sorption of some lanthanide on K^+-saturated marblehead illite: II. A multisite-surface complexation modeling[J]. Geochim Cosmochim Acta, 64: 195—213.

Lausen S K, Lindgreen H, Jakobsen H J *et al*., 1999. Solid-state ^{29}Si MAS NMR studies of illite and illite-smectite from shale[J]. Am Mineral, 84: 1443—1438.

Lazarev A N, 1972. Vibrational spectra and structure of silicates[M]. New York: Consultant Bureau.

Lippmaa E, Samoson A, Mägi M, 1986. High-resolution ^{27}Al NMR of aluminosilicate[J]. J Am Chem Soc, 108: 1730—1735.

Liu W X, Sun Z X, Du Q *et al*., 1999. A comparative study of surface acid-base characteristics of natural illites from different origins[J]. J Colloid Interface Sci, 219: 48—61.

Lu W P, Smith E H, 1996. Modeling potentiometric titration behavior of glauconite[J]. Geochim Cosmochim Acta, 60: 3363—3373.

Lützenkirchen J, 1999. The constant capacitance model and variable ionic strength: an evaluation of possible applications and applicability[J]. J Colloid Interface Sci, 217: 8—18.

Miyazaki A, Yokoyama T, 1999. Effects of anions on local structure of Al and Si in aluminosilicates[J]. J Colloid Interface Sci, 214: 395—399.

Nagy K L, 1995. Dissolution and precipitation kinetics of sheet silicates[M]. Chemical weathering rates of silicate minerals, reviews in mineralogy, Vol. 31(White A. F., Brantley S. L. eds.). Mineralogical Society of America. 173—233.

Nakamoto K, 1997. Infrared and Raman spectra of inorganic and coordination compounds, Part A: Theory and applications in inorganic chemistry, 5th edition[M]. New York: John Wiley & Sons Inc.

Sinitsyn V A, Aja S U, Kulik D A *et al*., 2000. Acid-base surface chemistry and sorption of some lanthanides on K^+-saturated marblehead illite: I. Results of an experimental investigation[J]. Geochim Cosmochim Acta, 64: 185—194.

Sjöberg S, 1998. Personal communication.

Smith K A, Kirkpatrick R J, Oldfield E *et al*., 1983. High resolution silicon-29 nuclear magnetic resonance spectroscopic study of rock-forming silicates[J]. Am Mineral, 68: 1206—1215.

Srodon J, 1984. *X*-ray powder diffraction identification of illite materials[J]. Clays Clay Minerals, 32: 337—349.

Tkàc I, Komadel P, Müller D, 1994. Acid-treated montmorillonites——a study by ^{29}Si and ^{27}Al MAS NMR[J]. Clay Minerals, 29: 11—19.

Weiss C A, Altaner S P, Kirkpatrick R J, 1987. High-resolution ^{29}Si NMR spectroscopy of 2:1 layer silicates: correlations among chemical shift, structural distortions, and chemical variations[J]. Am Mineral, 72: 935—942.

Westall J C, 1982. FITEQL: A computer program for determination chemical equilibrium constants from experiment data, version 2.0[R]. Report 82 - 02, Department of Chemistry, Oregon State University, Corvallis, OR, U. S. A.

(Received for review April 8, 2002. Accepted May 10,2002)